



Chaos properties of the one-dimensional long-range Ising spin-glass

Cécile Monthus, Thomas Garel

► **To cite this version:**

Cécile Monthus, Thomas Garel. Chaos properties of the one-dimensional long-range Ising spin-glass. *Journal of Statistical Mechanics*, 2014, 2014 (3), pp.20. <10.1088/1742-5468/2014/03/P03020>. <cea-01323269>

HAL Id: cea-01323269

<https://hal-cea.archives-ouvertes.fr/cea-01323269>

Submitted on 30 May 2016

HAL is a multi-disciplinary open access archive for the deposit and dissemination of scientific research documents, whether they are published or not. The documents may come from teaching and research institutions in France or abroad, or from public or private research centers.

L'archive ouverte pluridisciplinaire **HAL**, est destinée au dépôt et à la diffusion de documents scientifiques de niveau recherche, publiés ou non, émanant des établissements d'enseignement et de recherche français ou étrangers, des laboratoires publics ou privés.

Chaos properties of the one-dimensional long-range Ising spin-glass

Cécile Monthus and Thomas Garel

Institut de Physique Théorique, CNRS and CEA Saclay, 91191 Gif-sur-Yvette, France

For the long-range one-dimensional Ising spin-glass with random couplings decaying as $J(r) \propto r^{-\sigma}$, the scaling of the effective coupling defined as the difference between the free-energies corresponding to Periodic and Antiperiodic boundary conditions $J^R(N) \equiv F^{(P)}(N) - F^{(AP)}(N) \sim N^{\theta(\sigma)}$ defines the droplet exponent $\theta(\sigma)$. Here we study numerically the instability of the renormalization flow of the effective coupling $J^R(N)$ with respect to magnetic, disorder and temperature perturbations respectively, in order to extract the corresponding chaos exponents $\zeta_H(\sigma)$, $\zeta_J(\sigma)$ and $\zeta_T(\sigma)$ as a function of σ . Our results for $\zeta_T(\sigma)$ are interpreted in terms of the entropy exponent $\theta_S(\sigma) \simeq 1/3$ which governs the scaling of the entropy difference $S^{(P)}(N) - S^{(AP)}(N) \sim N^{\theta_S(\sigma)}$. We also study the instability of the ground state configuration with respect to perturbations, as measured by the spin overlap between the unperturbed and the perturbed ground states, in order to extract the corresponding chaos exponents $\zeta_H^{overlap}(\sigma)$ and $\zeta_J^{overlap}(\sigma)$.

I. INTRODUCTION

A. Chaos as instability of the renormalization flow

In the field of dynamical systems, the notion of chaos means ‘sensitivity to initial conditions’ and is quantified by the Lyapunov exponent $\lambda > 0$ which governs the exponential growth of the distance between two dynamical trajectories $\delta(t) \propto e^{\lambda t} \delta(0)$ that are separated by an infinitesimal distance $\delta(0)$ at time $t = 0$. In the field of spin-glasses, the notion of ‘chaos’ has been introduced as the sensitivity of the renormalization flow seen as a ‘dynamical system’, with respect to the initial conditions (the random couplings) or with respect to external parameters like the temperature T or the magnetic field H . On hierarchical lattices where explicit renormalization rules exist for the renormalized couplings J^R , the chaos properties have been thus much studied [1–10]. For other lattices without explicit renormalization rules, the droplet scaling theory [11–13] allows to define the chaos properties as follows :

(i) the effective renormalized coupling J^R of a d -dimensional disordered sample of linear size L containing $N = L^d$ spins can be defined as the difference between the free-energies $F^{(P)}(N)$ and $F^{(AP)}(N)$ corresponding to Periodic and Antiperiodic boundary conditions in the first direction respectively (the other $(d - 1)$ directions keep periodic boundary conditions)

$$J^R(N = L^d) \equiv F^{(P)}(N) - F^{(AP)}(N) = L^{\theta^{linear}} u = N^{\theta} u \quad (1)$$

where θ^{linear} is the usual droplet exponent associated to the linear size L , and where u is an $O(1)$ random variable of zero mean (with a probability distribution symmetric in $u \rightarrow -u$). In the following, we will use the droplet exponent $\theta = \theta^{linear}/d$ defined here with respect to the total number N of spins, in order to consider also fully connected models where the notion of length does not exist.

(ii) for the same disordered sample, one may now consider a perturbation δ (either in the disorder, temperature or magnetic field) and the corresponding renormalized coupling

$$J_{\delta}^R(N) \equiv F_{\delta}^{(P)}(N) - F_{\delta}^{(AP)}(N) \quad (2)$$

and construct the disorder-averaged correlation function

$$C_{\delta}(N) \equiv \frac{\overline{J^R(N) J_{\delta}^R(N)}}{\sqrt{\overline{(J^R(N))^2}} \sqrt{\overline{(J_{\delta}^R(N))^2}}} \quad (3)$$

The chaos exponent ζ_{δ} associated to the perturbation δ is then defined by the size dependence of the decorrelation scale at small perturbation δ

$$C_{\delta}(N) \underset{\delta \rightarrow 0}{\simeq} 1 - a(\delta N^{\zeta_{\delta}})^2 + o(\delta^2) \quad (4)$$

where a is a numerical constant. This method has been used to measure numerically the chaos exponents for spin-glasses on hypercubic lattices [2, 6, 14–16]. For each type of perturbation δ (magnetic, disorder, temperature), the droplet scaling theory predicts values of the corresponding chaos exponent ζ_{δ} [2, 13], as will be recalled below in the text.

B. Chaos as instability of the spin configurations

Besides the scaling droplet theory of spin-glasses recalled above, the alternative Replica-Symmetry-Breaking scenario [17] based on the mean-field fully connected Sherrington-Kirkpatrick model [18] considers that the main observable of the spin-glass phase is the overlap between configurations. As a consequence, another notion of chaos as been introduced [19–22] based on the overlap between the spins $S_i^{(0)}$ of the unperturbed system and the spins $S_i^{(\delta)}$ of the perturbed system

$$q_{(0,\delta)}(N) \equiv \frac{1}{N} \left| \sum_{i=1}^N S_i^{(0)} S_i^{(\delta)} \right| \quad (5)$$

The dimensionless ‘chaoticity parameter’ [21]

$$r_\delta(N) \equiv \frac{\overline{\langle q_{(0,\delta)}(N) \rangle}}{\sqrt{\overline{\langle q_{(0,0)}(N) \rangle}} \sqrt{\overline{\langle q_{(\delta,\delta)}(N) \rangle}}} \quad (6)$$

has been much studied in various spin-glass models [21–33] in order to extract the chaos exponent $\zeta_\delta^{overlap}$ that governs the size dependence of the decorrelation scale at small perturbation δ

$$r_\delta(N) \underset{\delta \rightarrow 0}{\simeq} 1 - b\delta N^{\zeta_\delta^{overlap}} + o(\delta) \quad (7)$$

where b is a numerical constant.

C. Organization of the paper

The aim of this work is to study the chaos properties of the one-dimensional long-range Ising spin-glass with respect to various perturbations, using the two procedures described above. The paper is organized as follows. In section II, we recall the properties of the one-dimensional long-range Ising spin-glass. The chaos exponents based on the correlation of Eq. 3 are studied for magnetic, disorder and temperature perturbations in sections III, IV and V respectively. The instability of the ground-state with respect to magnetic and disorder perturbations as measured by the chaoticity parameter of Eq. 6 is analyzed in section VI. Our conclusions are summarized in section VII. In Appendix A, we discuss the scaling of the lowest local field as a function of the system size, in order to interpret the results found in section VI.

II. REMINDER ON THE ONE-DIMENSIONAL LONG-RANGE ISING SPIN-GLASS

The one-dimensional long-range Ising spin-glass introduced in [34] allows to interpolate continuously between the one-dimensional nearest-neighbor model and the Sherrington-Kirkpatrick mean-field model [18]. Since it is much simpler to study numerically than hypercubic lattices as a function of the dimension d , this model has attracted a lot of interest recently [35–49] (here we will not consider the diluted version of the model [50]).

A. Definition of the model

The one-dimensional long-range Ising spin-glass [34] is defined by the Hamiltonian

$$\mathcal{H} = - \sum_{1 \leq i < j \leq N} J_{ij} S_i S_j \quad (8)$$

where the N spins $S_i = \pm 1$ lie periodically on a ring, so that the distance r_{ij} between the spins S_i and S_j reads [35]

$$r_{ij} = \frac{N}{\pi} \sin \left(|j - i| \frac{\pi}{N} \right) \quad (9)$$

The couplings are chosen to decay with respect to this distance as a power-law of exponent σ

$$J_{ij} = c_N(\sigma) \frac{\epsilon_{ij}}{r_{ij}^\sigma} \quad (10)$$

where ϵ_{ij} are random Gaussian variables of zero mean $\bar{\epsilon} = 0$ and unit variance $\overline{\epsilon^2} = 1$. The constant $c_N(\sigma)$ is defined by the condition [35]

$$1 = \sum_{j \neq 1} \overline{J_{1j}^2} = c_N^2(\sigma) \sum_{j \neq 1} \frac{1}{r_{1j}^{2\sigma}} \quad (11)$$

that ensures the extensivity of the energy. The exponent σ is thus the important parameter of the model.

B. Periodic versus Antiperiodic boundary conditions

For the long-range model of Eq. 8, 'Antiperiodic boundary conditions' means the following prescription [35] : for each disordered sample (J_{ij}) considered as 'Periodic', the 'Antiperiodic' consists in changing the sign $J_{ij} \rightarrow -J_{ij}$ for all pairs (i, j) where the shortest path on the circle goes through the bond $(L, 1)$.

C. Non-extensive region $0 \leq \sigma < 1/2$

In the non-extensive region $0 \leq \sigma < 1/2$, Eq. 11 yields

$$c_N(\sigma) \propto N^{\sigma - \frac{1}{2}} \quad (12)$$

so there is an explicit size-rescaling of the couplings as in the Sherrington-Kirkpatrick (SK) mean-field model [18] which corresponds to the case $\sigma = 0$. Recent studies [46, 47] have proposed that both universal properties like critical exponents, but also non-universal properties like the critical temperature do not depend on σ in the whole region $0 \leq \sigma < 1/2$, and thus coincide with the properties of the SK model $\sigma = 0$. For the SK model $\sigma = 0$, there seems to be a consensus on the shift exponent governing the correction to extensivity of the averaged value ground state energy [51–60]

$$\theta_{shift}(\sigma) \simeq 1/3 \quad (13)$$

The droplet exponent $\theta(\sigma)$ measured via Eq 1 in Ref [35] is indeed compatible with this constant value in the whole non-extensive region

$$\theta(0 \leq \sigma < 1/2) \simeq 1/3 \quad (14)$$

D. Extensive region $\sigma > 1/2$

In the extensive region $\sigma > 1/2$, Eq. 11 yields

$$c_N(\sigma) = O(1) \quad (15)$$

so that there is no size rescaling of the couplings. The limit $\sigma = +\infty$ corresponds to the nearest-neighbor one-dimensional model. The droplet exponent $\theta(\sigma)$ has been measured using Eq 1 via Monte-Carlo simulations on sizes $L \leq 256$ with the following results [35] (see [35] for other values of σ)

$$\begin{aligned} \theta(\sigma = 0.62) &\simeq 0.24 \\ \theta(\sigma = 0.75) &\simeq 0.17 \\ \theta(\sigma = 0.87) &\simeq 0.08 \\ \theta(\sigma = 1) &\simeq 0 \\ \theta(\sigma = 1.25) &\simeq -0.24 \end{aligned} \quad (16)$$

In our previous work [48], we have found that exact enumeration on much smaller sizes $6 \leq L \leq 24$ actually yield values close to Eq. 16.

There exists a spin-glass phase at low temperature for $\sigma < 1$ [34], characterized by a positive droplet exponent $\theta(\sigma) > 0$.

III. MAGNETIC FIELD CHAOS EXPONENT $\zeta_H(\sigma)$

In the presence of an external magnetic field H , the Hamiltonian of Eq. 8 becomes

$$\mathcal{H}_H = - \sum_{1 \leq i < j \leq N} J_{ij} S_i S_j - H \sum_{i=1}^N S_i \quad (17)$$

A. Scaling prediction of the droplet theory

Within the droplet scaling theory [12, 13], the chaos exponent associated to a magnetic field perturbation H can be predicted via the following Imry-Ma argument : the field H couples to the random magnetization of order $N^{1/2}$ of the extensive droplet of the unperturbed spin-glass state. The induced perturbation of order

$$\Delta_H(N) \propto HN^{1/2} \quad (18)$$

has to be compared with the renormalized coupling $J^R(N) \sim N^\theta u$ of Eq. 1. The appropriate scaling parameter is thus HN^{ζ_H} with the magnetic field chaos exponent

$$\zeta_H = \frac{1}{2} - \theta \quad (19)$$

B. Numerical results for the long-range Ising spin-glass

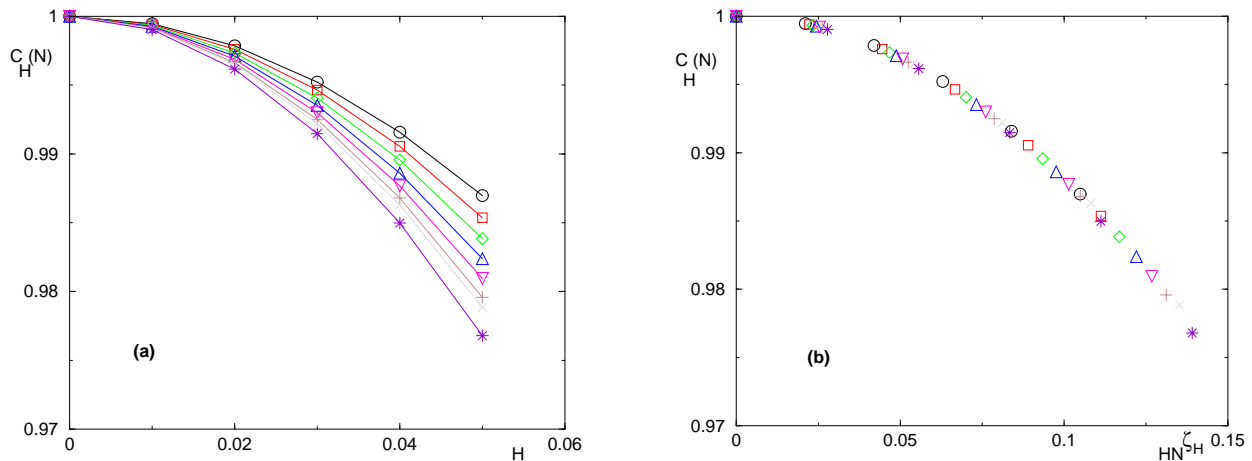


FIG. 1: Measure of the magnetic chaos exponent ζ_H for $\sigma = 0.75$: (a) Results for the correlation $C_H(N)$ as a function of the magnetic field $H = 0.01, 0.02, 0.03, 0.04, 0.05$ for various sizes $10 \leq N \leq 24$. (b) Same data as a function of the rescaled variable HN^{ζ_H} with $\zeta_H(\sigma = 0.75) \simeq 0.32$.

We have measured the correlation $C_H(N)$ of Eq. 3 at zero temperature $T = 0$, so that the free-energies F in Eq. 2 corresponds to the ground state energy E^{GS}

$$C_H(N) \equiv \frac{\left[E_{H=0}^{GS(P)}(N) - E_{H=0}^{GS(AP)}(N) \right] \left[E_H^{GS(P)}(N) - E_H^{GS(AP)}(N) \right]}{\sqrt{\left[E_{H=0}^{GS(P)}(N) - E_{H=0}^{GS(AP)}(N) \right]^2} \sqrt{\left[E_H^{GS(P)}(N) - E_H^{GS(AP)}(N) \right]^2}} \quad (20)$$

The ground state energies $E_H^{GS(P)}(N)$ and $E_H^{GS(AP)}(N)$ corresponding to Periodic or Antiperiodic boundary conditions for various values of the external magnetic field H have been measured via exact enumeration of the 2^N spin configurations for small even sizes $10 \leq N \leq 24$. The statistics over samples have been obtained for instance with the following numbers $n_s(N)$ of disordered samples

$$n_s(L \leq 10) = 10^9; \dots; n_s(L = 16) = 53.10^5; \dots; n_s(L = 24) = 12 \times 10^3 \quad (21)$$

We have used five small values of the magnetic field $H = 0.01, 0.02, 0.03, 0.04, 0.05$ in order to extract the chaos exponent from the expansion (Eq 4)

$$C_H(N) \underset{\delta \rightarrow 0}{\simeq} 1 - a_{\text{magnetic}}(HN^{\zeta_H})^2 + o(H^2) \quad (22)$$

where a_{magnetic} is a numerical constant. As an example, we show on Fig. 1 our data for $\sigma = 0.75$.

In the non-extensive region $0 \leq \sigma < 1/2$, our numerical results are compatible with the value given by Eqs 14 and 19

$$\zeta_H(0 \leq \sigma < 1/2) = \frac{1}{2} - \theta(0 \leq \sigma < 1/2) \simeq \frac{1}{6} \simeq 0.17 \quad (23)$$

In the extensive region, our numerical measures as a function of σ

$$\begin{aligned} \zeta_H(\sigma = 0.62) &\simeq 0.26 \\ \zeta_H(\sigma = 0.75) &\simeq 0.32 \\ \zeta_H(\sigma = 0.87) &\simeq 0.39 \\ \zeta_H(\sigma = 1) &\simeq 0.47 \\ \zeta_H(\sigma = 1.25) &\simeq 0.64 \end{aligned} \quad (24)$$

are in reasonable agreement with the formula of Eq. 19 and the values of the droplet exponent $\theta(\sigma)$ recalled in Eq 16.

IV. DISORDER CHAOS EXPONENT $\zeta_J(\sigma)$

For each realization of the couplings of Eq. 10, we draw independent Gaussian random variables ϵ'_{ij} of zero mean and unit variance, and we consider the following perturbation of amplitude δ of the couplings of Eq. 10

$$J_{ij}^{(\delta)} = c_N(\sigma) \frac{\left(\frac{\epsilon_{ij} + \delta \epsilon'_{ij}}{\sqrt{1 + \delta^2}}\right)}{r_{ij}^\sigma} \quad (25)$$

A. Scaling prediction of the droplet theory

Within the droplet scaling theory [12, 13], the chaos exponent associated to a disorder perturbation for *short-range* spin-glasses can be predicted via the following Imry-Ma argument : the disorder perturbation of amplitude δ which couples to the *surface of dimension* d_s of the extensive droplet

$$\Delta_J^{SR}(N) \propto \delta L^{\frac{d_s}{2}} = \delta N^{\frac{d_s}{2d}} \quad (26)$$

has to be compared with the renormalized coupling $J^R(N) \sim N^\theta u$ of Eq. 1. The appropriate scaling parameter is thus δN^{ζ_J} with the disorder chaos exponent

$$\zeta_J^{SR} = \frac{d_s}{2d} - \theta \quad (27)$$

For the long-range one-dimensional model, the scaling of the induced perturbation has to be re-evaluated from the following double sum involving one point i in the droplet D and one point j outside the droplet D

$$\Delta_J^{LR}(N) \propto \delta c_N(\sigma) \sqrt{\sum_{i \in D} \sum_{j \notin D} \frac{1}{|i - j|^{2\sigma}}} \quad (28)$$

In the non-extensive regime $\sigma < 1/2$, the sum is dominated by the large distances $|i - j|$, so that taking into account Eq. 12, Eq. 28 behaves as

$$\Delta_J^{(0 \leq \sigma < 1/2)}(N) \propto \delta c_N(\sigma) \sqrt{N^{2-2\sigma}} = \delta N^{\frac{1}{2}} \quad (29)$$

yielding the chaos exponent

$$\zeta_J^{(0 \leq \sigma < 1/2)} = \frac{1}{2} - \theta(\sigma) \quad (30)$$

In the extensive regime $\sigma > 1/2$, the sum of Eq. 28 is dominated by the short distances in $|i - j|$, so that one recovers the scaling of Eq. 27

$$\zeta_J^{\sigma > 1/2} = \frac{d_s(\sigma)}{2} - \theta(\sigma) \quad (31)$$

where the surface dimension $d_s(\sigma)$ is expected to vary between $d_s(\sigma = 1/2) = 1$ to match the non-extensive regime of Eq. 30, and $d_s(\sigma \rightarrow +\infty) = 0$ to match the exact result of the one-dimensional nearest-neighbor model [2].

B. Numerical results for the long-range Ising spin-glass

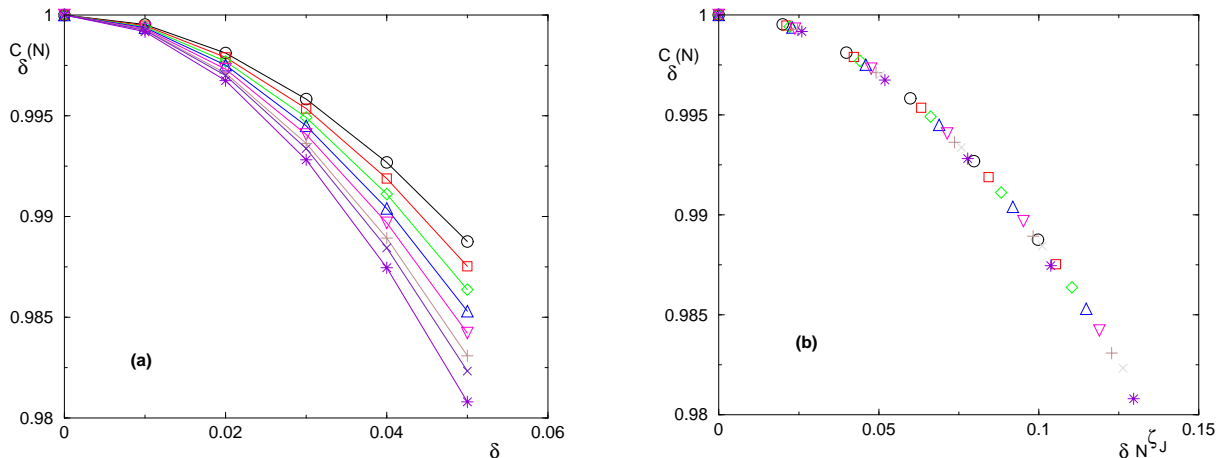


FIG. 2: Measure of the disorder chaos exponent ζ_J for $\sigma = 0.75$: (a) Results for the correlation $C_\delta(N)$ as a function of the amplitude $\delta = 0.01, 0.02, 0.03, 0.04, 0.05$ of the perturbation (Eq. 25) for various sizes $10 \leq N \leq 24$. (b) Same data as a function of the rescaled variable δN^{ζ_J} with $\zeta_J(\sigma = 0.75) \simeq 0.3$.

We have measured the correlation $C_\delta(N)$ of Eq. 3 at zero temperature $T = 0$, so that the free-energies F in Eq. 2 corresponds to the ground state energy E^{GS}

$$C_\delta(N) \equiv \frac{\overline{[E_{\delta=0}^{GS(P)}(N) - E_{\delta=0}^{GS(AP)}(N)] [E_\delta^{GS(P)}(N) - E_\delta^{GS(AP)}(N)]}}{\sqrt{[E_{\delta=0}^{GS(P)}(N) - E_{\delta=0}^{GS(AP)}(N)]^2} \sqrt{[E_\delta^{GS(P)}(N) - E_\delta^{GS(AP)}(N)]^2}} \quad (32)$$

The ground state energies corresponding to Periodic or Antiperiodic boundary conditions for various values of the perturbation amplitude δ of Eq. 25 have been measured via exact enumeration of the 2^N spin configurations for small even sizes $10 \leq N \leq 24$, with a statistics similar to Eq. 21. We have used five small values of the amplitude $\delta = 0.01, 0.02, 0.03, 0.04, 0.05$ in order to extract the chaos exponent from the expansion (Eq 4)

$$C_\delta(N) \underset{\delta \rightarrow 0}{\simeq} 1 - a_{disorder}(\delta N^{\zeta_J})^2 + o(\delta^2) \quad (33)$$

where $a_{disorder}$ is a numerical constant. As an example, we show on Fig. 2 our data for $\sigma = 0.75$.

In the non-extensive region $0 \leq \sigma < 1/2$, our numerical results are compatible with the value given by Eqs 14 and 30

$$\zeta_J(0 \leq \sigma < 1/2) = \frac{1}{2} - \theta(0 \leq \sigma < 1/2) \simeq \frac{1}{6} \simeq 0.17 \quad (34)$$

In the extensive region $\sigma > 1/2$, our numerical measures

$$\begin{aligned} \zeta_J(\sigma = 0.62) &\simeq 0.26 \\ \zeta_J(\sigma = 0.75) &\simeq 0.3 \\ \zeta_J(\sigma = 0.87) &\simeq 0.33 \\ \zeta_J(\sigma = 1) &\simeq 0.36 \\ \zeta_J(\sigma = 1.25) &\simeq 0.44 \end{aligned} \quad (35)$$

yield the following estimations for the surface dimension $d_s(\sigma) = 2(\theta(\sigma) + \zeta_J(\sigma))$ of extensive droplets (Eq 31)

$$\begin{aligned}
 d_s(\sigma = 0.62) &\simeq 1 \\
 d_s(\sigma = 0.75) &\simeq 0.94 \\
 d_s(\sigma = 0.87) &\simeq 0.82 \\
 d_s(\sigma = 1) &\simeq 0.72 \\
 d_s(\sigma = 1.25) &\simeq 0.4
 \end{aligned}
 \tag{36}$$

C. Finite disorder perturbation

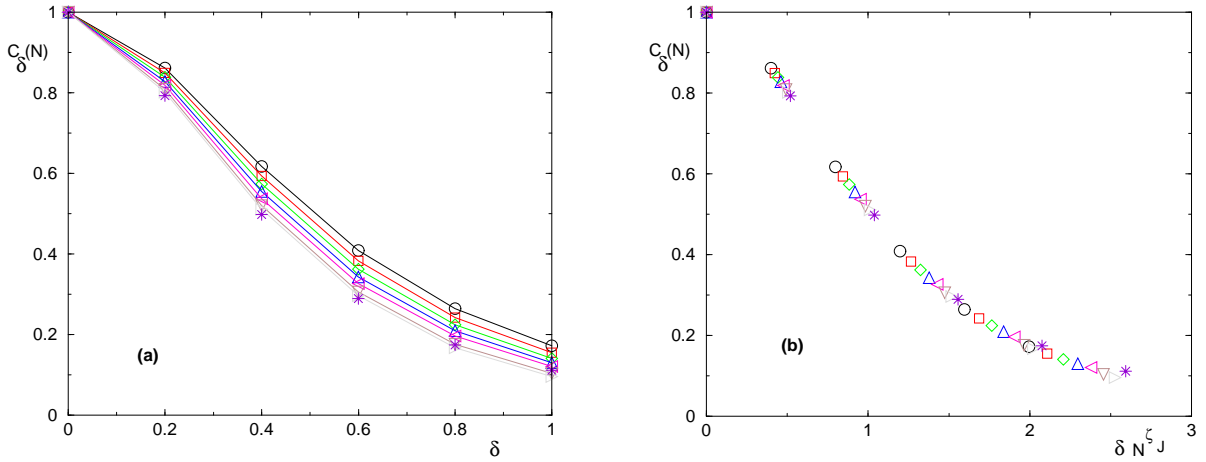


FIG. 3: Disorder perturbation of finite amplitude δ for $\sigma = 0.75$: (a) Results for the correlation $C_\delta(N)$ as a function of the amplitude $\delta = 0.2, 0.4, 0.6, 0.8, 1$. of the perturbation (Eq. 25) for various sizes $10 \leq N \leq 24$. (b) Same data as a function of the rescaled variable δN^{ζ_J} with $\zeta_J(\sigma = 0.75) \simeq 0.3$.

We have also study numerically disorder perturbation (Eq. 25) with a finite amplitude δ . As shown on Fig. 3 for $\sigma = 0.75$, we find that the chaos exponent extracted from the expansion of Eq. 33 for small amplitude δ , allows to rescale also the results for finite δ .

V. TEMPERATURE CHAOS EXPONENT $\zeta_T(\sigma)$

A. Scaling prediction of the droplet theory

Within the droplet scaling theory [12, 13], the chaos exponent associated to a temperature perturbation δT for *short-range* spin-glasses can be predicted via the following Imry-Ma argument : the perturbation actually involves the same scaling as Eq. 26, as a consequence of the scaling the entropy of extensive droplets as $L^{\frac{d_s}{2}}$ (coming from some Central Limit Theorem for independent local contributions along the interface)

$$\Delta_T^{SR}(N) \propto (\delta T) L^{\frac{d_s}{2}} = (\delta T) N^{\frac{d_s}{2d}}
 \tag{37}$$

The comparison with the renormalized coupling $J^R(N) \sim N^\theta u$ of Eq. 1 yields that the appropriate scaling parameter is $(\delta T) N^{\zeta_T}$ with the temperature chaos exponent

$$\zeta_T^{SR} = \frac{d_s}{2d} - \theta
 \tag{38}$$

that coincides with the disorder chaos exponent of Eq. 27.

For the one-dimensional long-range model, the argument about independent local contributions along the interface leading to Eq. 37 cannot be used anymore, and we have thus studied numerically the scaling of the entropy of droplets via the difference of entropy between Periodic and Antiperiodic Boundary conditions

$$S^{DW}(N) \equiv S^{(P)}(N) - S^{(AP)}(N) \sim N^{\theta_{s\nu}}
 \tag{39}$$

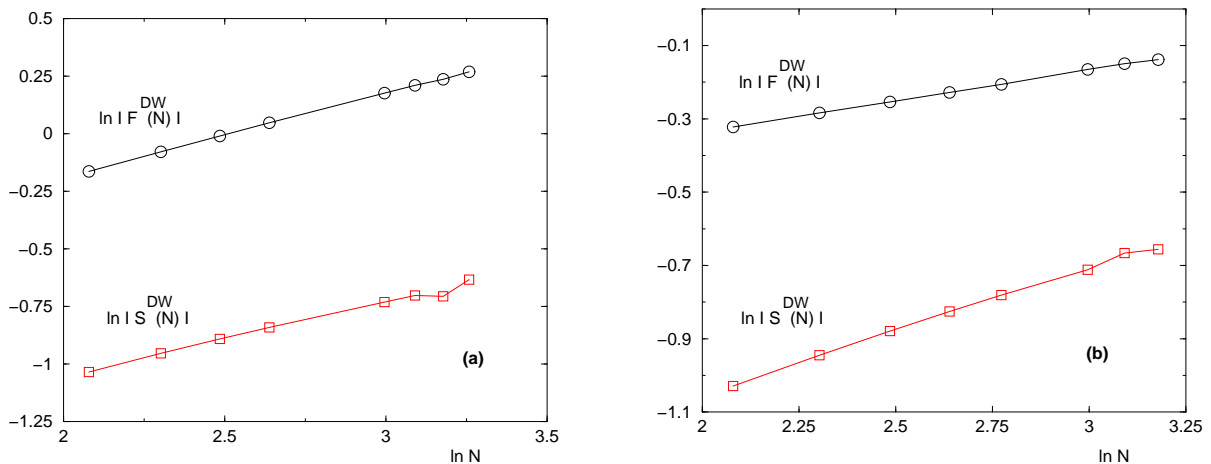


FIG. 4: Comparison between the scaling of the Domain-Wall free-energy $F^{DW}(N)$ (Eq. 40) and the Domain-Wall entropy $S^{DW}(N)$ (Eq. 39) at temperature $T = 0.05$ in log-log plots : (a) for $\sigma = 0.25$ in the non-extensive region, the two slopes coincide $\theta(\sigma = 0.25) \simeq 1/3 \simeq \theta_S(\sigma = 0.25)$. (b) for $\sigma = 0.75$ in the extensive region, the droplet exponent $\theta(\sigma = 0.75) \simeq 0.17$ for the free-energy is smaller than the entropy exponent $\theta_S(\sigma = 0.75) \simeq 0.33$.

(where v is an $O(1)$ random variable of zero mean) that defines the entropy exponent θ_S . It should be compared with the droplet exponent θ that governs the free-energy difference of Eq. 1

$$F^{DW}(N) \equiv F^{(P)}(N) - F^{(AP)}(N) \sim N^{\theta} u \quad (40)$$

As examples, we shown on Fig. 4 our results for $\sigma = 0.25$ and $\sigma = 0.75$. Our conclusions are the following :

(i) we find that the entropy exponent $\theta_S(\sigma)$ takes the simple value

$$\theta_S(\sigma) \simeq \frac{1}{3} \quad (41)$$

for all σ . This is actually consistent with the same constant value found recently for the dynamical barrier exponent $\psi(\sigma) \simeq \frac{1}{3}$ [49] (see [61] for the conjecture on the relation between θ_S and ψ).

(ii) in the non-extensive region $0 \leq \sigma < 1/2$ (see Fig. 4 (a)), the entropy exponent of Eq. 41 coincides with the droplet exponent

$$\theta_S(\sigma < 1/2) \simeq \frac{1}{3} = \theta(\sigma < 1/2) \quad (42)$$

so that the corresponding temperature chaos exponent actually vanishes

$$\zeta_T(\sigma < 1/2) = 0 \quad (43)$$

(iii) in the extensive region $\sigma > 1/2$ where the droplet exponent is smaller $\theta(\sigma) < 1/3$

$$\theta_S(\sigma > 1/2) \simeq \frac{1}{3} > \theta(\sigma > 1/2) \quad (44)$$

this means that there exists an entropy-energy cancellation mechanism as in short-ranged models [12, 13], and that the corresponding temperature chaos exponent is positive

$$\zeta_T(\sigma > 1/2) = \frac{1}{3} - \theta(\sigma > 1/2) > 0 \quad (45)$$

B. Numerical results for the long-range Ising spin-glass

We have measured the following correlation (Eq. 3) to study temperature perturbations with respect to zero-temperature

$$C_T(N) \equiv \frac{\overline{[F_{T=0}^{(P)}(N) - F_{T=0}^{(AP)}(N)]} \overline{[F_T^{(P)}(N) - F_T^{(AP)}(N)]}}{\sqrt{\overline{[F_{T=0}^{(P)}(N) - F_{T=0}^{(AP)}(N)]^2}} \sqrt{\overline{[F_T^{(P)}(N) - F_T^{(AP)}(N)]^2}}} \quad (46)$$

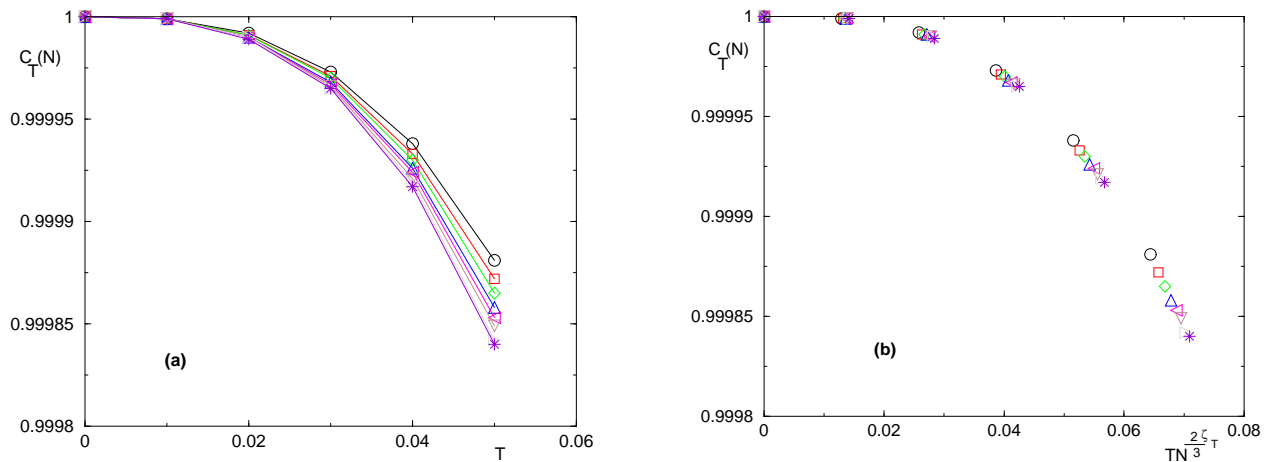


FIG. 5: Measure of the temperature chaos exponent ζ_T for $\sigma = 0.75$: (a) Results for the correlation $C_T(N)$ as a function of the temperature $T = 0.01, 0.02, 0.03, 0.04, 0.05$ for various sizes $10 \leq N \leq 24$. (b) Same data as a function of the rescaled variable $TN^{2/3}\zeta_T$ (see Eq. 47) with $\zeta_T(\sigma = 0.75) \simeq 0.17$.

via exact enumeration of the 2^N spin configurations for small even sizes $10 \leq N \leq 24$, with a statistics similar to Eq. 21. We have used five small values of the temperature $T = 0.01, 0.02, 0.03, 0.04, 0.05$ in order to extract the temperature chaos exponent from the expansion

$$C_T(N) \underset{T \rightarrow 0}{\simeq} 1 - a_{\text{temperature}} T (TN^{\zeta_T})^2 + o(T^3) \quad (47)$$

where $a_{\text{temperature}}$ is a numerical constant. Note the additional prefactor of T with respect to the standard quadratic expansion of Eq. 4 that can be explained from the behavior of the entropy near zero-temperature [6]. As an example, we show on Fig. 5 our data for $\sigma = 0.75$.

In the non-extensive regime $0 \leq \sigma < 1/2$, we find that the temperature chaos exponent vanishes

$$\zeta_T(0 \leq \sigma < 1/2) \simeq 0 \quad (48)$$

in agreement with Eq. 43.

In the extensive region $\sigma > 1/2$, our numerical measures

$$\begin{aligned} \zeta_T(\sigma = 0.62) &\simeq 0.09 \\ \zeta_T(\sigma = 0.75) &\simeq 0.17 \\ \zeta_T(\sigma = 0.87) &\simeq 0.26 \\ \zeta_T(\sigma = 1) &\simeq 0.36 \\ \zeta_T(\sigma = 1.25) &\simeq 0.58 \end{aligned} \quad (49)$$

are in agreement with Eq. 45.

VI. INSTABILITY OF THE GROUND STATE WITH RESPECT TO PERTURBATIONS

In this section, we describe our numerical results concerning the chaoticity parameter of Eq. 6 at zero temperature $T = 0$ to characterize the instability of the ground-state S_i^{GS} with respect to a perturbation δ via the overlap (Eq. 5)

$$q_{(0,\delta)}^{(T=0)}(N) \equiv \frac{1}{N} \left| \sum_{i=1}^N S_i^{GS(0)} S_i^{GS(\delta)} \right| \quad (50)$$

Since there is no thermal fluctuations at zero temperature, the denominator of Eq. 6 is unity, so that the chaoticity parameter of Eq. 6 reduces to the disorder-average of Eq. 50

$$r_{\delta}^{(T=0)}(N) \equiv \overline{q_{(0,\delta)}^{(T=0)}(N)} \quad (51)$$

A. Magnetic perturbation at zero temperature

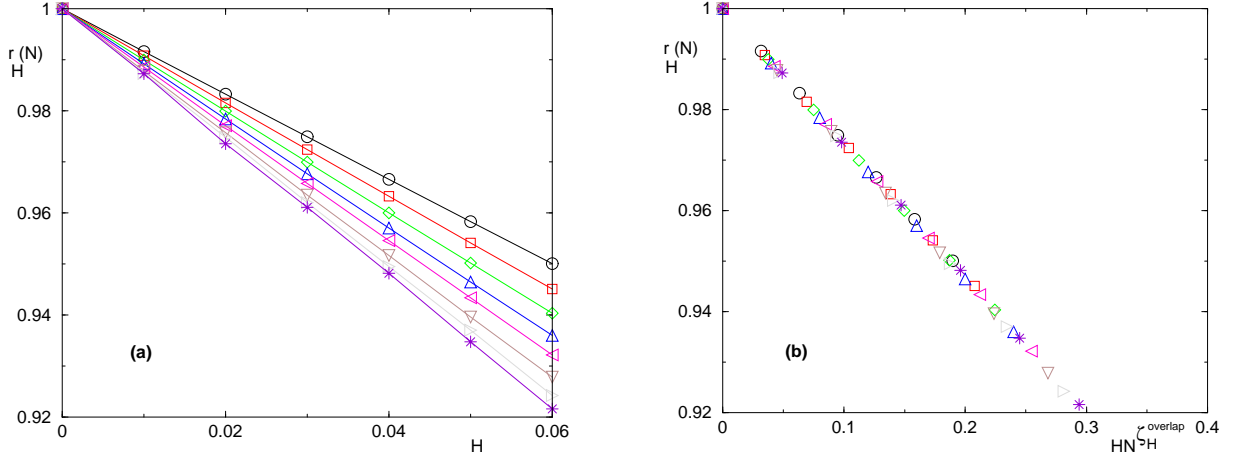


FIG. 6: Measure of the chaos exponent $\zeta_H^{overlap}$ for $\sigma = 0.75$: (a) Results for the chaoticity parameter $r_H^{(T=0)}(N)$ as a function of the external magnetic field $H = 0.01, 0.02, 0.03, 0.04, 0.05, 0.06$ for various sizes $10 \leq N \leq 24$. (b) Same data as a function of the rescaled variable $HN^{\zeta_H^{overlap}}$ with $\zeta_H^{overlap}(\sigma = 0.75) \simeq 0.5$.

We have measured the chaoticity parameter $r_H^{(T=0)}(N)$ of Eq. 51. The ground state configurations of the spins have been obtained via exact enumeration of the 2^N spin configurations for small even sizes $10 \leq N \leq 24$. The statistics over samples is similar to Eq. 21. We have used six small values of the magnetic field $H = 0.01, 0.02, 0.03, 0.04, 0.05, 0.06$ in order to extract the chaos exponent from the expansion of Eq. 7

$$r_H(N) \underset{H \rightarrow 0}{\simeq} 1 - b_{magnetic} H N^{\zeta_H^{overlap}} + o(H) \quad (52)$$

where $b_{magnetic}$ is a numerical constant.

As an example, we show on Fig. 6 our data for $\sigma = 0.75$ leading to

$$\zeta_H^{overlap}(\sigma = 0.75) \simeq 0.5 \quad (53)$$

in agreement with [39] (see Fig. 4 of [39]). For $\sigma = 0$ corresponding to the mean-field SK model, we also find the same value

$$\zeta_H^{overlap}(\sigma = 0) \simeq 0.5 \quad (54)$$

in agreement with [19, 23, 39] (although the other value $\zeta_H^{overlap}(\sigma = 0) \simeq 3/8$ can be found in [20, 21, 23, 27]).

B. Disorder perturbation at zero temperature

For the disorder perturbation of Eq. 25, we have measured the chaoticity parameter $r_\delta^{(T=0)}(N)$ of Eq. 51. The ground state configurations of the spins have been obtained via exact enumeration of the 2^N spin configurations for small even sizes $10 \leq N \leq 24$. The statistics over samples is similar to Eq. 21. We have used six small values of the perturbation amplitude $\delta = 0.01, 0.02, 0.03, 0.04, 0.05, 0.06$ in order to extract the chaos exponent from the expansion of Eq. 7

$$r_\delta(N) \underset{\delta \rightarrow 0}{\simeq} 1 - b_{disorder} \delta N^{\zeta_J^{overlap}} + o(\delta) \quad (55)$$

where $b_{disorder}$ is a numerical constant.

As an example, we show on Fig. 7 our data for $\sigma = 0.75$ leading to

$$\zeta_J^{overlap}(\sigma = 0.75) \simeq 0.5 \quad (56)$$

For $\sigma = 0$ corresponding to the mean-field SK model, we also find the same value

$$\zeta_J^{overlap}(\sigma = 0) \simeq 0.5 \quad (57)$$

in agreement with [22, 29, 31].

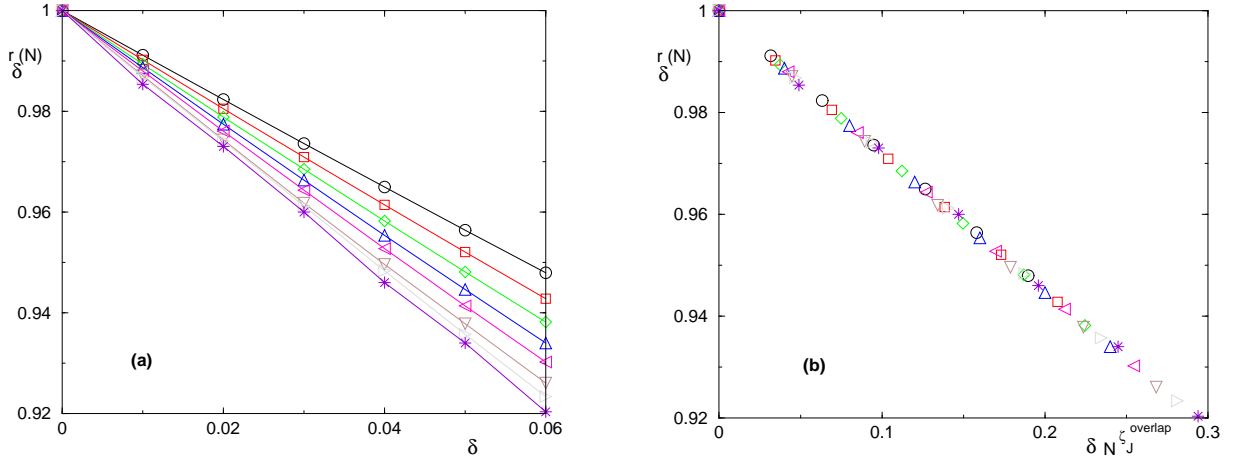


FIG. 7: Measure of the chaos exponent $\zeta_J^{overlap}$ for $\sigma = 0.75$: (a) Results for the chaoticity parameter $r_{\delta}^{(T=0)}(N)$ as a function of the amplitude $\delta = 0.01, 0.02, 0.03, 0.04, 0.05, 0.06$ of the disorder perturbation (Eq. 25) for various sizes $10 \leq N \leq 24$. (b) Same data as a function of the rescaled variable $\delta N^{\zeta_J^{overlap}}$ with $\zeta_J^{overlap}(\sigma = 0.75) \simeq 0.5$.

C. Explanation in terms of the avalanche triggered by the lowest local field

For the mean-field SK model corresponding to $\sigma = 0$, the results of Eqs 54 and 57 simply reflect the scaling of the lowest local field $h_{min}(N) \propto N^{-1/2}$ (see Eq. A6 and explanations in Appendix A), since the flipping of the spin corresponding to this lowest local field is known to be able to trigger an extensive avalanche [29, 62–64].

Our numerical results of Eq. 53 and 56 for $\sigma = 0.75$ also coincide with the scaling of the lowest local field $h_{min}(N) \propto N^{-1/2}$ (see Eq. A7 and Figure 8 in Appendix A). Our conclusion is thus that for $\sigma = 0.75$ also, the flipping of the spin corresponding to the lowest local field is able to trigger an extensive avalanche.

Note that this is very different from the nearest-neighbor model defined on hypercubic lattices : the flipping of the lowest local field $h_{min}(N) \propto N^{-1} = L^{-d}$ (See Eq. A4 and explanations in Appendix A) is not able to trigger an extensive avalanche. And the overlap chaos exponents which have been measured in finite d with respect to the linear size L are of order $\zeta_J^{overlap}(d=2) \simeq 1$ [24, 29] and $\zeta_J^{overlap}(d=3) \simeq 1.1$ [29, 30, 33] and are thus much smaller than the value d which would correspond to the scaling of the lowest local field $h_{min} = L^{-d}$.

VII. CONCLUSION

For the long-range one-dimensional Ising spin-glass with random couplings decaying as $J(r) \propto r^{-\sigma}$, we have studied numerically the chaos properties as a function of σ for various types of perturbation near the zero-temperature fixed point.

We have first studied the instability of the renormalization flow of the effective coupling defined as the difference between the free-energies corresponding to Periodic and Antiperiodic boundary conditions $J^R(N) \equiv F^{(P)}(N) - F^{(AP)}(N)$:

(a) for magnetic perturbations, we have found that the magnetic chaos exponents satisfies the standard droplet formula (Eq. 19) involving the droplet exponent $\theta(\sigma)$

$$\zeta_H(\sigma) = \frac{1}{2} - \theta(\sigma) \quad (58)$$

(b) for disorder perturbation, we have measured the disorder chaos exponent $\zeta_J(\sigma)$, which yields the surface dimension $d_s(\sigma)$ of droplets via the standard droplet formula

$$\zeta_J(\sigma) = \frac{d_s(\sigma)}{2} - \theta(\sigma) \quad (59)$$

(c) for temperature perturbation, we have obtained that the temperature chaos exponent $\zeta_T(\sigma)$ satisfies the formula

$$\zeta_T(\sigma) = \frac{1}{3} - \theta(\sigma) \quad (60)$$

where $1/3 = \theta_S(\sigma) = \psi(\sigma)$ is the entropic exponent $\theta_S(\sigma)$, and also the barrier exponent $\psi(\sigma)$ of the dynamics.

Then we have also studied the instability of the ground state configuration with respect to perturbations, as measured by the spin overlap between the unperturbed and the perturbed ground states. Both for magnetic and disorder perturbations, we have obtained for all σ the exponent

$$\zeta_H^{overlap}(\sigma) = \frac{1}{2} = \zeta_J^{overlap}(\sigma) \quad (\text{A1})$$

which simply reflects the scaling of the lowest local field (Eq. A7) that can trigger an extensive avalanche.

For all these cases, we have discussed the similarities and differences with short range models in finite dimension d .

Appendix A: Scaling of the lowest local field $h_{min}(N)$ at zero temperature

From the probability distribution $P_N(h)$ of the local field

$$h_i \equiv \left| \sum_j J_{ij} S_j^{(0)} \right| \quad (\text{A1})$$

seen by spins in the ground-state of a spin-glass model of N sites, the typical lowest local field $h_{min}(N)$ in a sample can be estimated from

$$\frac{1}{N} = \int_0^{h_{min}(N)} dh P_N(h) \quad (\text{A2})$$

1. Finite dimension with nearest-neighbor interaction

For nearest-neighbor spin-glass models defined on hypercubic lattices in dimension $d > 1$, the probability distribution $P_N(h)$ has a finite weight at $h = 0$ in the thermodynamic limit [65]

$$P_\infty^{(d)}(h = 0) > 0 \quad (\text{A3})$$

so that the lowest local field scales as (Eq. A2)

$$h_{min}^{(d)}(N) \simeq \frac{1}{N P_{N=\infty}(h = 0)} \quad (\text{A4})$$

2. Mean-field SK model

For the mean-field SK model, the probability distribution $P_{N=\infty}(h)$ vanishes linearly [66, 67]

$$P_{N=\infty}^{(SK)}(h) \underset{h \rightarrow 0}{\propto} h \quad (\text{A5})$$

so that Eq. A2 implies the scaling

$$h_{min}^{(SK)}(N) \propto \frac{1}{N^{\frac{1}{2}}} \quad (\text{A6})$$

3. Long-range one-dimensional spin-glass model

For the long-range one-dimensional spin-glass model, the probability distribution $P_N(h)$ has been studied numerically in [65]. Since the behavior of the histogram $P_N(h)$ near $h = 0$ is difficult to extrapolate [65], we have chosen instead to study directly the lowest local field h_{min} via exact enumeration of the ground states on the sizes $6 \leq N \leq 26$. As shown on Fig. 8 for the case $\sigma = 0.75$, we find the scaling analogous to Eq. A6 for all values of $\sigma \geq 0$

$$h_{min}^{(\sigma)}(N) \propto \frac{1}{N^{\frac{1}{2}}} \quad (\text{A7})$$

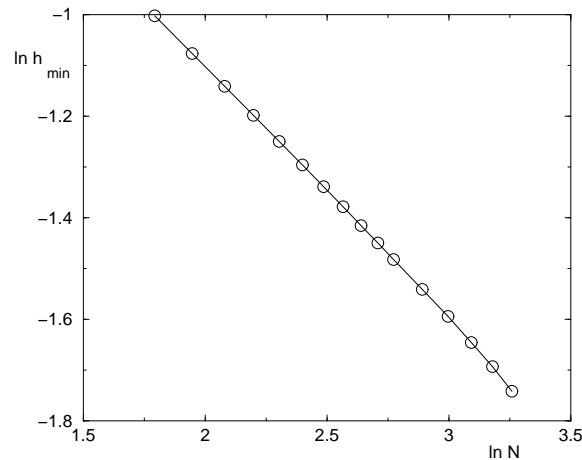


FIG. 8: Scaling of the lowest local field $h_{min}(N)$ in the ground state for $\sigma = 0.75$ as a function of the system size N : the log-log plot corresponds to the slope -0.5 , i.e. to the scaling of Eq. A7.

Note that for the histogram, this corresponds to the finite-size behavior

$$P_N^{(\sigma)}(h = 0) \propto \frac{1}{N^{\frac{1}{2}}} \quad (\text{A8})$$

via Eq. A2.

-
- [1] S.R. McKay, A.N. Berker and S. Kirkpatrick, Phys. Rev. Lett. 48, 767 (1982);
A.N. Berker and S.R. McKay, J. Stat. Phys. 36, 787 (1984);
S.R. McKay and A.N. Berker, J. Appl. Phys. 55, 1646 (1984);
N. Aral and A.N. Berker, Phys. Rev. B 79, 014434 (2009).
- [2] A. J. Bray and M.A. Moore, Phys. Rev. Lett. 58, 57 (1987).
- [3] J.R. Banavar and A.J. Bray, Phys. Rev. B 35, 8888 (1987).
- [4] B. Sundaram, M. Cieplak and J.R. Banavar, Phys. Rev. A 41, 5713 (1990).
- [5] M. Nifle and H.J. Hilhorst, Phys. Rev. Lett. 68, 2992 (1992);
M. Ney-Nifle and H.J. Hilhorst, Physica A 193, 48 (1993);
M. Ney-Nifle and H.J. Hilhorst, Physica A 194, 462 (1993);
M.J. Thill and H.J. Hilhorst, J. Phys. I France 6, 67 (1996).
- [6] T. Aspelmeier, A.J. Bray and M.A. Moore, Phys. Rev. Lett. 89, 197202 (2002).
- [7] M. Sasaki and O.C. Martin, Phys. Rev. Lett. 91, 097201 (2003).
- [8] F. Krzakala, Europhys. Lett. 66, 847 (2004).
- [9] T. Jorg and F. Krzakala, J. Stat. Mech. L01001 (2012).
- [10] S.T.O. Almeida, E.M.F. Curado and F.D. Nobre, J. Stat. Mech. P06013 (2013).
- [11] W.L. Mc Millan, J. Phys. C 17, 3179 (1984).
- [12] A.J. Bray and M. A. Moore, J. Phys. C 17 (1984) L463;
A.J. Bray and M. A. Moore, “Scaling theory of the ordered phase of spin glasses” in Heidelberg Colloquium on glassy dynamics, edited by JL van Hemmen and I. Morgenstern, Lecture notes in Physics vol 275 (1987) Springer Verlag, Heidelberg.
- [13] D.S. Fisher and D.A. Huse, Phys. Rev. Lett. 56, 1601 (1986) ; Phys. Rev. B 38, 373 (1988) ; Phys. Rev. 38, 386 (1988).
- [14] M. Sasaki, K. Hukushima, H. Yoshino and H. Takayama, Phys. Rev. Lett. 95, 267203 (2005);
M. Sasaki, K. Hukushima, H. Yoshino and H. Takayama, Phys. Rev. Lett. 99, 137202 (2007).
- [15] J. Lukic, E. Marinari, O.C. Martin and S. Sabatini, J. Stat. Mech. L10001 (2006).
- [16] C.K. Thomas, D.A. Huse and A.A. Middleton, arXiv:1012.3444; C.K. Thomas, D.A. Huse and A.A. Middleton, Phys. Rev. Lett. 107, 047203 (2011).
- [17] M. Mézard, G. Parisi and M.A. Virasoro, World Scientific (1987), “Spin glass theory and beyond”, and references therein.
- [18] D. Sherrington and S. Kirkpatrick, Phys. Rev. Lett. 35, 1792 (1975).
- [19] G. Parisi, Physica 124A, 523 (1984).
- [20] I. Kondor, J. Phys. A Math. Gen. 22, L163 (1989);
I. Kondor and A. Vesgo, J. Phys. A Math. Gen. 26, L641 (1993).

- [21] F. Ritort, Phys. Rev. B 50, 6844 (1994).
- [22] V. Azcoiti, E. Follana and F. Ritort, J. Phys. A Math Gen 28, 3863 (1995).
- [23] S. Franz and M. Ney-Nifle, J. Phys. A 28, 2499 (1995).
- [24] H. Rieger, L. Santen, U. Blasum, M. Diehl, M. Junger and G. Rinaldi, J. Phys. A Math. Gen. 29, 3939 (1996).
- [25] M. Ney-Nifle and A.P. Young, J. Phys. A Math. Gen. 30, 5311 (1997);
M. Ney-Nifle, Phys. Rev. B 57, 492 (1998).
- [26] A. Billoire and E. Marinari, J. Phys. A 33 L265 (2000);
A. Billoire and E. Marinari, Europhys. Lett. 60, 775 (2002).
- [27] A. Billoire and B. Coluzzi, Phys. Rev. E 67, 036108 (2003).
- [28] T. Rizzo and A. Crisanti, Phys. Rev. Lett. 90, 137201 (2003).
- [29] F. Krzakala and J.P. Bouchaud, Europhys. Lett. 72, 472 (2005).
- [30] H.G. Katzgraber and F. Krzakala, Phys. Rev. Lett. 98, 017201 (2007).
- [31] T. Aspelmeier, Phys. Rev. Lett. 100, 117205 (2008);
T. Aspelmeier, J. Phys. A 41, 205005 (2008);
T. Aspelmeier, J. Stat. Mech. P04018 (2008).
- [32] G. Parisi and T. Rizzo, J. Phys. A 43, 235003 (2010).
- [33] L.A. Fernandez, V. Martin-Mayor, G. Parisi and B. Seoane, arXiv:1307.2361.
- [34] G. Kotliar, P.W. Anderson and D.L. Stein, Phys. Rev. B 27, 602 (1983).
- [35] H.G. Katzgraber and A.P. Young, Phys. Rev. B 67, 134410 (2003).
- [36] H.G. Katzgraber and A.P. Young, Phys. Rev. B 68, 224408 (2003).
- [37] H.G. Katzgraber, M. Korner, F. Liers and A.K. Hartmann, Prog. Theor. Phys. Sup. 157, 59 (2005).
- [38] H.G. Katzgraber, M. Korner, F. Liers, M. Junger and A.K. Hartmann, Phys. Rev. B 72, 094421 (2005).
- [39] H.G. Katzgraber, J. Phys. Conf. Series 95, 012004 (2008).
- [40] H. G. Katzgraber and A. P. Young, Phys. Rev. B 72, 184416 (2005).
- [41] A.P. Young, J. Phys. A 41, 324016 (2008).
- [42] H. G. Katzgraber, D. Larson and A. P. Young, Phys. Rev. Lett. 102, 177205 (2009).
- [43] M.A. Moore, Phys. Rev. B 82, 014417 (2010).
- [44] H.G. Katzgraber, A.K. Hartmann and and A.P. Young, Physics Procedia 6, 35 (2010).
- [45] H.G. Katzgraber and A.K. Hartmann, Phys. Rev. Lett. 102, 037207 (2009);
H.G. Katzgraber, T. Jorg, F. Krzakala and A.K. Hartmann, Phys. Rev. B 86, 184405 (2012).
- [46] T. Mori, Phys. Rev. E 84, 031128 (2011).
- [47] M. Wittmann and A. P. Young, Phys. Rev. E 85, 041104 (2012)
- [48] C. Monthus and T. Garel, arXiv:1306.0423.
- [49] C. Monthus and T. Garel, arXiv:1309.2154.
- [50] L. Leuzzi, G. Parisi, F. Ricci-Tersenghi and J.J. Ruiz-Lorenzo, Phys. Rev. Lett. 101, 107203 (2008);
L. Leuzzi, G. Parisi, F. Ricci-Tersenghi and J.J. Ruiz-Lorenzo, Phys. Rev. Lett. 103, 267201 (2009);
A. Sharma and A.P. Young, Phys. Rev. B 84, 014428 (2011);
R.A. Banos, L. A. Fernandez, V. Martin-Mayor, A. P. Young, Phys. Rev. B 86, 134416 (2012) ;
D. Larson, H.G. Katzgraber, M.A. Moore and A.P. Young, Phys. Rev. B 87, 024414 (2013).
- [51] A. Andreev, F. Barbieri and O.C. Martin, Eur. Phys. J. B 41, 365 (2004).
- [52] J.-P. Bouchaud, F. Krzakala and O.C. Martin, Phys. Rev. B 68, 224404 (2003).
- [53] M. Palassini, arxiv:cond-mat/0307713; J. Stat. Mech. P10005 (2008).
- [54] T. Aspelmeier, M.A. Moore and A.P. Young, Phys. Rev. Lett. 90, 127202 (2003); T. Aspelmeier, Phys. Rev. Lett. 100, 117205 (2008); T. Aspelmeier, J. Stat. Mech. P04018 (2008).
- [55] H.G. Katzgraber, M. Korner, F. Liers, M. Junger and A.K. Hartmann, Phys. Rev. B 72, 094421 (2005).
- [56] M. Korner, H.G. Katzgraber, and A.K. Hartmann, J. Stat. Mech. P04005 (2006).
- [57] T. Aspelmeier, A. Billoire, E. Marinari and M.A. Moore, J. Phys. A Math. Theor. 41 , 324008 (2008).
- [58] S. Boettcher, J. Stat. Mech. P07002 (2010).
- [59] C. Monthus and T. Garel, J. Stat. Mech. P01008 (2008).
- [60] C. Monthus and T. Garel, J. Stat. Mech. P02023 (2010).
- [61] C. Monthus and T. Garel, J. Phys. A Math. Gen. 41, 115002 (2008).
- [62] F. Pazmandi, G. Zarland, and G. T. Zimanyi, Phys. Rev. Lett. 83, 1034 (1999);
F. Pazmandi and G. T. Zimanyi, arXiv:0903.4235.
- [63] P. Le Doussal, M. Muller and K.J. Wiese, Euro. Phys. Lett. 91, 57004 (2010);
P. Le Doussal, M. Muller and K.J. Wiese, Phys. Rev. B 85, 214402 (2012).
- [64] J. C. Andresen, Z. Zhu, R. S. Andrist, H.G. Katzgraber, V. Dobrosavljevic and G. T. Zimanyi, Phys. Rev. Lett. 111, 097203 (2013).
- [65] S. Boettcher, H.G. Katzgraber and D. Sherrington, J. Phys. A Math. Gen. 41, 324007 (2008).
- [66] D.J. Thouless, P.W. Anderson and R.G. Palmer, Phil. Mag. 35, 593 (1977).
- [67] R.G. Palmer and C.M. Pond, J. Phys. F Met. Phys. 9, 1451 (1979).